

Testing Inter-event Times Moments as Earthquake Precursory Signals



A. Talbi

*Earthquake Research Institute, University of Tokyo, Japan
Centre de Recherche en Astronomie Astrophysique et Geophysique CRAAG, Algiers, Algeria*

K. Nanjo & K. Satake

Earthquake Research Institute, University of Tokyo, Japan

J. Zhuang

Institute of Statistical Mathematics, Tokyo, Japan

M. Hamdache

Centre de Recherche en Astronomie Astrophysique et Geophysique CRAAG, Algiers, Algeria

SUMMARY:

This study introduces the ratio of the first to second order moments of earthquake inter-event times, namely moment's ratio (MR), as a precursory alarm function to forecast large earthquakes in Japan. The use of MR is motivated by its ability to characterize long term changes in background seismicity which may be anomalous before large events. In a retrospective test of $M \geq 7$ target earthquakes, the forecasting performance of MR is evaluated using Molchan diagrams. The results show good performance of MR forecasts at long and intermediate terms. In particular, MR maps predict 15 of the 18 shallow earthquakes occurred in the testing region during the last two decades with an alarm rate of about 20%. In addition, MR reduces the missing rate of shallow events by about 60 % comparing to the relative intensity method, and succeeds in predicting the 2011 Mw 9.0 Tohoku earthquake while the RI method fails.

Keywords: Earthquake forecasting · Inter-event times · Alarm function · Molchan diagrams

1. INTRODUCTION

One of the main purposes of seismology is to answer the question when (time), where (location) and how big (size) next large earthquake is. Since the focus is large events above a given threshold magnitude, the answer is based on forecast in space and time. Earthquake prediction evolved from several attempts that tried to answer such question (e.g. Keilis-Borok 2002). Nowadays seismicity based forecasting methods, such as the pattern informatics (PI) and the relative intensity (RI) methods (Tiampo et al. 2002), are promising tools to tackle earthquake prediction issues. The PI method uses a measure to detect seismic quiescence and activation. The RI method assumes earthquakes to occur likely in the regions of high past seismicity. Both methods use the probability estimates of past seismicity to forecast next target earthquakes with superior size. The changes in the background seismicity, which may be observed before the occurrence of large events (quiescence or activation), is a precursory variable used implicitly by a number of earthquake forecasting methods, for example the PI and RI methods. However, the estimation of background seismicity is problematic, since each forecasting method uses its own ingredients in the estimation of background seismicity rate. This suggests that one way to improve forecasting is to provide better evaluation of background seismicity changes. Following this motivation, this study uses the ratio of the mean over the variance of inter-event times, called hereafter moment ratio MR as precursory alarm function to forecast earthquakes with magnitude $M \geq 7$ ($M7+$) in Japan. The MR statistic was carried out by fitting local inter-event times using a Gamma distribution (Corral 2003). Later, it was found to provide a non-parametric estimate of the proportion background events in the whole catalog (Hainzl et al. 2006).

The objective in this study is to test the MR forecasts, and compare their performance to the RI method.

RI provides a suitable reference model for comparison in the absence of significant performance gain of other methods (Zechar and Jordan 2008, Nanjo 2010). The performance of MR forecasts is evaluated by using Molchan error diagrams (Molchan and Keilis-Borok 2008, Molchan 2010). In the following, three retrospective tests are performed to evaluate the forecasting ability of the proposed MR method at long and intermediate terms, and to discuss the prediction of the 2011 M_w 9.0 Tohoku earthquake at short term. It is found that MR forecasts performs very well and outscore the RI method. In particular, MR succeeds to predict the Tohoku earthquake while the RI method fails.

2. DATA AND METHOD

A composite catalog covering all Japan during the period 679-2011 is compiled, by combining the Utsu historical seismicity records for the period 679-1922 and the Japan Meteorological Agency (JMA) catalog for the period 1923-2011. This catalog is used in test 1 (long term forecasting), while for test 2 (intermediate term forecasting) and test 3 (short term forecasting for the Tohoku earthquake), the catalog data are updated to the end of March 2012. The JMA catalog used contain preliminary determined epicenters starting from September 2011. The learning period starts January 1st 1890 whereas it ends 7 days before a reference M7+ earthquake depending on the test. Earthquakes with magnitude $M \geq 6$ (M6+) occurred during the learning period are used to calculate the MR and RI alarm functions which are then used to forecast M7+ target earthquakes.

Inter-event times are sampled using the earthquake random sampling (ERS) algorithm (Talbi and Yamazaki 2010) with fixed sampling radius $r = 100$ km. For each sampling disk centred on x , a series of inter-event times $\{\xi_i\}_{i=1}^n$ is obtained. The moment ratio score MR is calculated for each location x as,

$$MR(x, r) = MR(x) = \frac{\bar{\xi}}{\sigma_{\xi}^2} \quad (3.1)$$

where $\bar{\xi}$ and σ_{ξ}^2 are the arithmetic mean and the variance of the time series $\{\xi_i\}_{i=1}^n$. The obtained MR scores from all sampling disks are plotted on a regular grid with cell size $0.5^\circ \times 0.5^\circ$. The set of grid cells with at least one observed MR score value defines the testing region G . For each cell C , the MR alarm function P_{MR} is defined as the maximum observed MR score from all locations x occurring inside the cell C ,

$$P_{MR}(C) = \max_{x \in C} [MR(x)] \quad (3.2)$$

P_{MR} is divided by the maximum observed score $P_{MR}^{max} = \max_{C \in G} [P_{MR}(C)]$, to restrict its range to $[0, 1]$. The alarm function P_{RI} for RI is calculated similarly using the relative frequency of the M6+ events.

We proceed by retrospective binary forecasting. The testing region G is subdivided into m sub-regions G_i (here $G = \cup_{i=1}^m C_i$ where C_i are the cells forming the testing region), while the testing period $[0, T]$ is divided into S sub-periods of equal length Δt . For each $t > 0$, a strategy π_i is defined inside each space-time region $C_i \times [t, t + \Delta t]$ as follows (Molchan 2010),

$$\pi_i(t) = \begin{cases} 1 & \text{if an alarm is declared in the region } C_i \times [t, t + \Delta t] \\ 0 & \text{if not} \end{cases} \quad (3.3)$$

If N target events occurs in the testing region $G \times [0, T]$, we can calculate the statistics a : Number of target earthquakes that occurred in alarm cells, b : Number of alarm cells with no target earthquakes, c : Number of target earthquakes occurred outside alarm cells, d : Number of non-alarm cells with no target earthquakes. Two types of diagrams are used to evaluate our forecasts. The first one, which is called the receiver operating characteristic (ROC) diagram, plots the hit rate $H = a/(a+c)$ against the false alarm rate $F = b/(b+d)$. Points above the diagonal $H = F$ outscore the random guessing strategy (Jolliffe and Stephenson 2003). The second diagram which is called error or Molchan diagram

(Molchan 1997), plots the miss rate $\nu = c/(a+c) = 1-H$ against the space-time alarm rate $\tau = (a+b)/(a+b+c+d)$. The diagonal $\tau + \nu = 1$ corresponds to trivial strategies of random guess, and any points significantly below this diagonal outscore the random guessing strategy defined here by the score P_U . In this sense, Molchan diagram is used to demonstrate how far from a random guessing are predictions that result from a given algorithm. Namely, it is used in this study to evaluate MR and RI forecasts by testing the null hypothesis $H_0 : P_{MR} = P_U$ (respectively (resp.) $H_0 : P_{RI} = P_U$) against the alternative $H_1 : P_{MR} > P_U$ (resp. $H_1 : P_{RI} > P_U$). Recently, Molchan diagram has been generalized to evaluate how far is the prediction from a given referential model (Molchan and Keilis-Borok 2008, Molchan 2010). In both cases, the miss rate is plotted against the following weighted space-time alarm rate,

$$\tau_w = \sum_{i=1}^m w_i \tau_i \quad (3.4)$$

where τ_i is the alarm time rate in the testing region C_i ,

$$\tau_i = \frac{1}{s} \sum_{j=1}^{s-1} \mathbf{1}_{\{\pi_i(j\Delta t)=1\}} \quad (3.5)$$

The logical function $\mathbf{1}_A$ equals 1 if A is true and 0 otherwise.

To obtain a diagonal corresponding to the random guessing strategy, we use a uniform spatial prior distribution which assigns equal weights $w_i = w_i^U = 1/m$ to all cells C_i in Eqn. 3.4. To simplify the notation, we write $\tau_w = \tau$. In the special case where the weights in Eqn. 3.4 are equal to the unknown normalized rate of target events $w_i = w_i^{RI} = n_i/N$, with n_i the number of target events occurred in the testing region C_i , all RI reference strategies are projected onto the diagonal $\nu + \tau_w = 1$ of random guessing. However, the RI method uses estimates of normalized rate from learning events with magnitude lower than target events, so that RI strategies define a domain around the diagonal. Namely Molchan diagram is used in this case to test the null hypothesis $H_0 : P_{MR} = P_{RI}$ against the alternative $H_1 : P_{MR} > P_{RI}$. In the following, Molchan diagram is plotted for each test using successively the weights w_i^U and w_i^{RI} in Eqn. 3.4, to evaluate the MR forecasting performance comparing to random guess and the RI method, respectively.

In this study, the optimal MR forecast maps are obtained by plotting the MR scores exceeding the alarm function threshold corresponding to the minimum forecasting error $e(\tau, \nu) = \tau + \nu$. The minimal forecasting error $e(\tau, \nu) = \tau + \nu$ is obtained by maximizing Peirce Skill score $SS_p(\tau, \nu) = 1 - \nu - \tau$ (Tiampo and Shcherbakov 2012),

$$\min_{(\tau, \nu) \in [0,1]^2} \{e(\tau, \nu)\} = \text{Max}_{(\tau, \nu) \in [0,1]^2} (SS_p(\tau, \nu)) \quad (3.6)$$

Optimal RI maps are obtained by plotting RI scores with a space time alarm rate equivalent to the corresponding MR optimal maps. In the following tests, the choice of the learning and testing periods is based on maximizing data quantity and quality.

3. RESULTS

3.1. Test 1 (Long term forecasting)

For this test, the learning period is January 1st 1890– January 8th 1993 and the testing period is January 8th 1993–December 31st 2011. There are 22 M7+ target earthquakes (Table 1) occurred in the testing region composed of 282 cells. Events n^o 1, 5, 7 and 17 are deep (depth ≥ 100 km). About 1500 M6+ earthquakes were used in the calculation of the MR and RI alarm functions, among which 1115 occurred in the testing region. Here the alarm time step is the whole testing period $\Delta t \approx 19$ years.

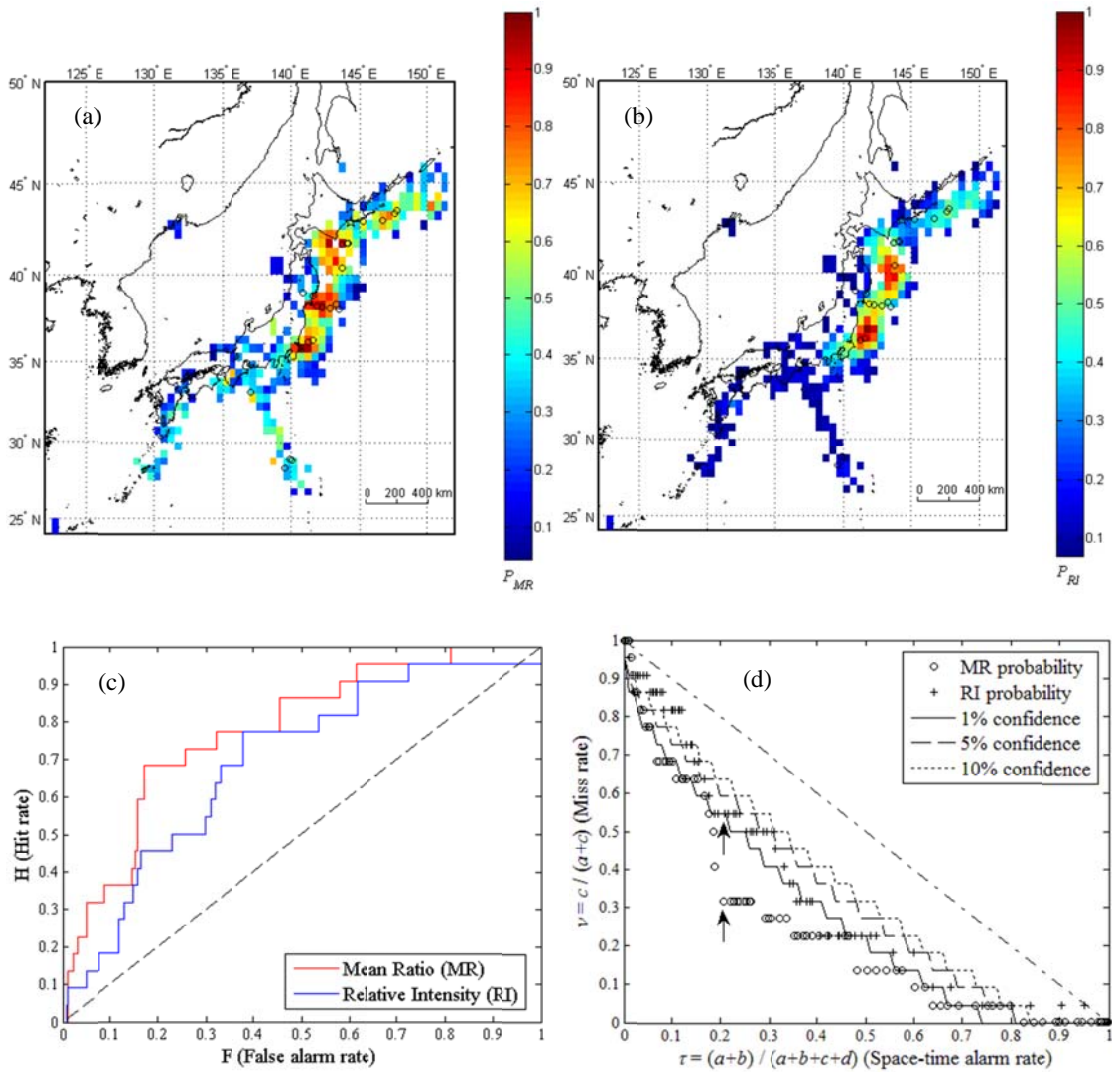
Table 1. List of target M7+ earthquakes occurred in the testing region during the testing period for test 1 and 3. Long, Lat and Mag denote longitude, latitude and magnitude respectively.

ID	Long	Lat	Date	Mag	Name/Region	Cluster	Test n ^o
1	144.353	42.920	1993/01/15	7.5	Kushiro-oki	C ₃	1
2	147.673	43.375	1994/10/04	8.2	Hokkaido-touhou-oki	C ₃	1
3	147.802	43.558	1994/10/09	7.3	Hokkaido-touhou-oki aftershock	C ₃	1
4	143.745	40.430	1994/12/28	7.6	Sanriku-haruka-oki	C ₂	1
5	139.912	28.891	1998/08/20	7.1	Chichi jima	C ₅	1
6	146.744	43.008	2000/01/28	7.0	Nemuro-oki	C ₃	1
7	140.086	28.821	2000/08/06	7.2	Chichi jima	C ₅	1
8	141.651	38.821	2003/05/26	7.1	Miyagi-ken-oki	C ₁	1
9	144.078	41.779	2003/09/26	8.0	Tokachi-oki	C ₂	1
10	143.691	41.710	2003/09/26	7.1	Tokachioki aftershock	C ₂	1
11	137.141	33.138	2004/09/05	7.4	Kii-hanto-oki	–	1
12	145.275	42.946	2004/11/29	7.1	Kushiro-oki	C ₃	1
13	142.278	38.150	2005/08/16	7.2	Miyagi-ken-oki	C ₁	1
14	141.608	36.228	2008/05/08	7.0	Ibaraki-ken-oki	C ₄	1
15	140.881	39.030	2008/06/14	7.2	Iwate-Miyagi nairiku	–	1
16	144.152	41.776	2008/09/11	7.1	Tokachi-oki aftershock	C ₂	1
17	139.589	28.358	2010/11/30	7.1	Chichi jima	C ₅	1
18	143.280	38.328	2011/03/09	7.3	Tohoku foreshock	C ₁	1 and 3
19	142.861	38.103	2011/03/11	9.0	Tohokuchiho-Taiheiyo-oki	C ₁	1 and 3
19p	142.781	39.839	2011/03/11	7.4	Tohoku aftershock	–	3
20	141.265	36.108	2011/03/11	7.6	Tohoku aftershock	C ₄	1 and 3
21	141.920	38.204	2011/04/07	7.2	Tohoku aftershock	C ₁	1 and 3
22	143.507	38.032	2011/07/10	7.3	Tohoku aftershock	C ₁	1 and 3
23	138.566	31.428	2012/01/01	7.0	Torishima Kinkai	–	3

Fig 1a and b show the MR and RI maps, respectively. Hot spots in the MR map are broader and include the region below latitude 35° N; whereas the RI map is more cool with only two big hot spots. Hot spots in the MR map allow us to identify 5 clusters (Table 1). Namely, the MR map hot spots catch the central cluster C₁ (n° 8, 13, 18, 19, 21 and 22) including Miyagi-ken-oki and Tohoku earthquakes. The same occurs for the cluster C₂ formed by the Tokachi-oki and its aftershocks (n° 9, 10 and 16), and the Sanriku-haruka-oki earthquake (n° 4). The cluster C₃ located east of Hokkaido formed by Kushiro-oki, Hokkaido-touhou-oki and Nemuro-oki (n° 1, 2, 3, 6 and 12) is also marked by hot spots. The maximum MR value is registered at the east of Tokyo bay where the cluster C₄ formed by the Ibaraki-ken-oki and an aftershock of Tohoku earthquake occurred (n° 14 and 20). The southern cluster C₅ formed by Chichi jima deep (depth > 400 km) earthquakes (n° 5, 7 and 17) and the Kii-hanto-oki (n° 11) occurs close to hot cells. The proximity of target earthquakes from hot cells suggests that our prediction may be improved by smoothing via Moore neighborhood, for example by considering the eight cells around each hot cell (Moore neighborhood) as alarm cells. The Iwate-Miyagi-Nairiku (n° 15) did not occur at hot spots probably because its epicentral region is not well covered by our sparse data. The RI map shows mainly two hot spots. The northern one is concentrated around the Sanriku-haruka-oki (n° 4), and the second one, which spots the cluster C₄, is located around the Ibaraki-ken-oki and an aftershock of the Tohoku earthquake (n° 14 and 20). The cluster C₁ which includes the Tohoku earthquake is not highlighted by any hot spot but appears as an extension or junction between the two former hot spots.

Fig. 1c shows the ROC diagram for MR and RI. The dashed diagonal line is for random guessing. Both forecasting methods outperform the random guessing especially MR. Fig 1d and e show Molchan diagram obtained using a uniform and RI weighted spatial prior respectively. Solid, dashed and dotted curves shows 1%, 5% and 10% critical boundaries. The arrows points to the minimal forecasting error of MR (Eqn. 3.5) and the corresponding RI forecast. Since points below the critical boundaries reject the null hypothesis, we can conclude from Fig. 1d that MR (resp. RI) outcores the random guessing at the test level $\alpha = 1\%$ for $\tau \in [0.18, 0.67]$ (resp. $\tau \in [0.35, 0.46]$) and at $\alpha = 5\%$ for almost all τ (resp. for $\tau \in [0.16, 0.80]$). Similarly, Fig. 1e shows MR outscoring RI at $\alpha = 1\%$ and 5%

for $\tau \in [0.25, 0.42]$ and $\tau \in [0.26, 0.55]$ respectively. Fig. 1f shows Peirce skill score for the diagram in Fig. 1d. The maximum $SS_p^{\max} = SS_p(0.2057, 0.3182)$ is reached for a threshold $c_0 = 0.6085$. Fig. 1g and h show optimal forecast maps for MR and RI respectively. The optimal MR map is plotted using 58 cells with $MR \geq c_0$. The alarm rate is $\tau = (58/282) = 0.2057$ with 7 earthquakes missing from 22. The optimal RI map is plotted using 59 cells with $RI \geq 0.4697$, i.e., a spatial extent equivalent to the former MR map in Fig. 1g. The alarm rate is $\tau = (59/282) = 0.2092$. The miss rate is about twice higher comparing to the optimal MR map, with 12 earthquakes missing. RI miss rate is about three times higher than MR if only shallow earthquakes (depth < 100 km) are considered (8/18 vs. 3/18).



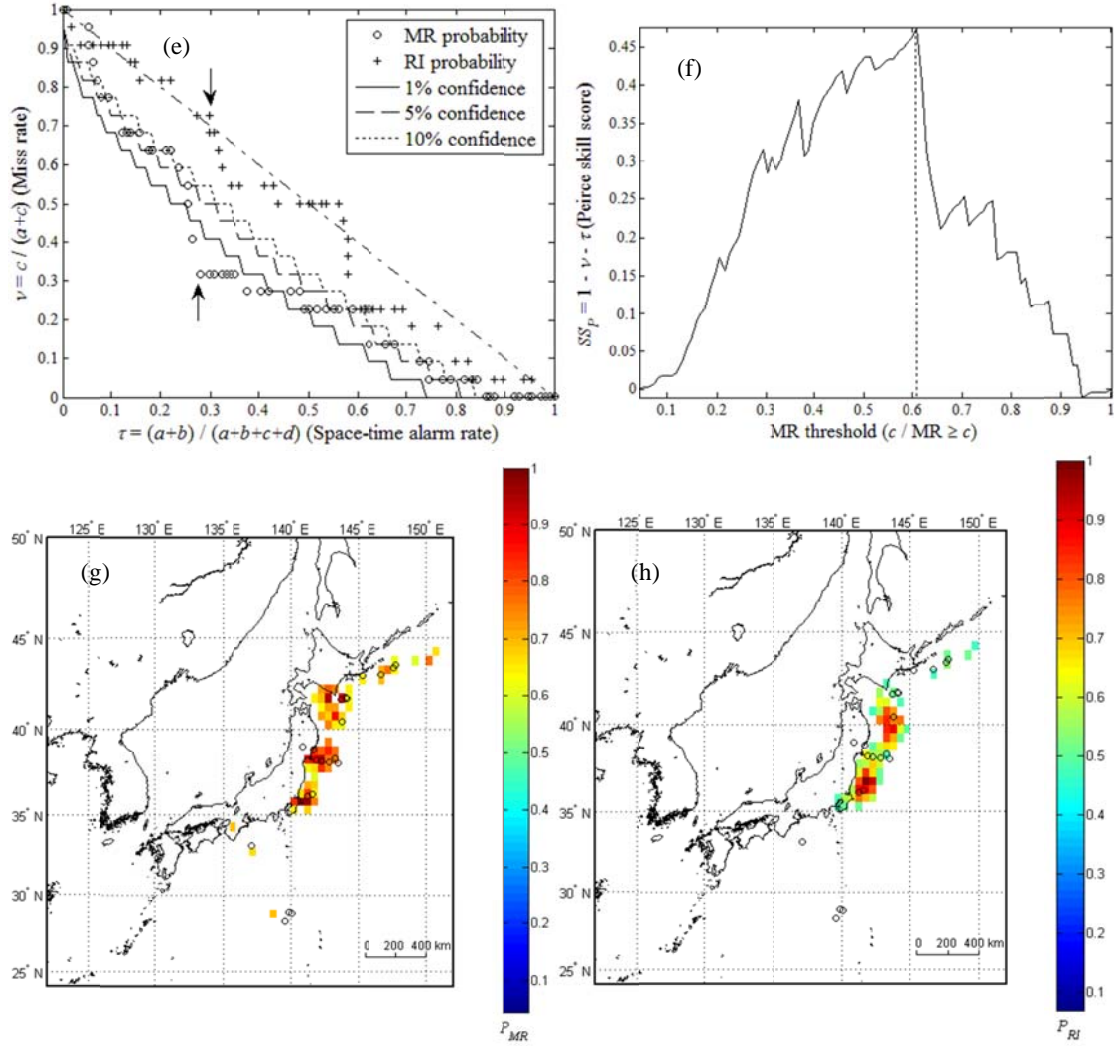


Figure 1. (a) MR and (b) RI forecast maps for the testing period 1993–2011. The circles and the star show the M7+ events occurred in the testing region. The distribution is plotted 7 days before the reference earthquake shown as a star marker ($n^{\circ} 1$) using M6+ events occurred between 1890 and 1993. (c) ROC diagram for the MR and RI methods. (d–e) Molchan error diagram for test 1 obtained using (d) uniform and (e) RI weighted spatial priors. (f) Peirce Skill Score for Molchan diagram in Fig. 1d. (g–h) Optimal (g) MR and (h) RI forecast maps corresponding to the arrows in Fig. 1d. The star and the Chichi jima cluster in the south are deep missed events.

3.2. Test 2 (Intermediate term forecasting)

For this test, the learning period is January 1st 1890–March 14th 1982 and the testing period is March 14th 1982–March 31st 2012. There are 29 M7+ target events occurring in the testing region which consists of 271 cells. In total, 1354 M6+ events were used in the calculation of the MR and RI alarm functions, from which 987 occurred in the testing region during the learning period. Here the alarm time step is $\Delta t \approx 3$ years. MR and RI scores are updated in each step, and the alarm declaration is decided accordingly. This allows us to test the performance of the proposed MR method at intermediate term, and the obtained results reflect the mean performance of forecasting in the three years following the release of the maps.

Fig. 2a and b show Molchan diagram for the uniform and the RI weighted spatial priors, respectively. In Fig. 2a, MR and RI outscore random guess at $\alpha = 1\%$ and 5% , respectively, for some alarm rate ranges. For Fig. 2b, MR outscores RI at $\alpha = 10\%$ and 5% for $\tau \in [0.37, 0.75]$ and $\tau \in [0.54, 0.68]$, respectively.

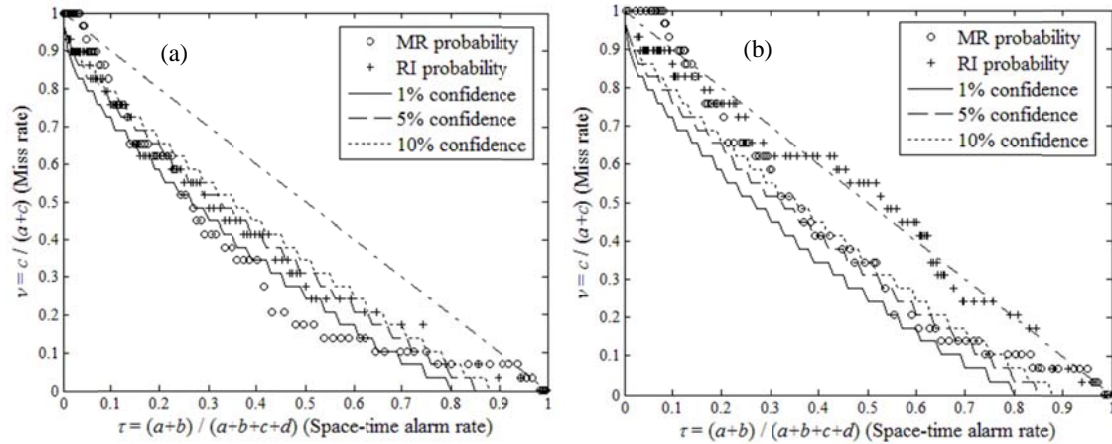
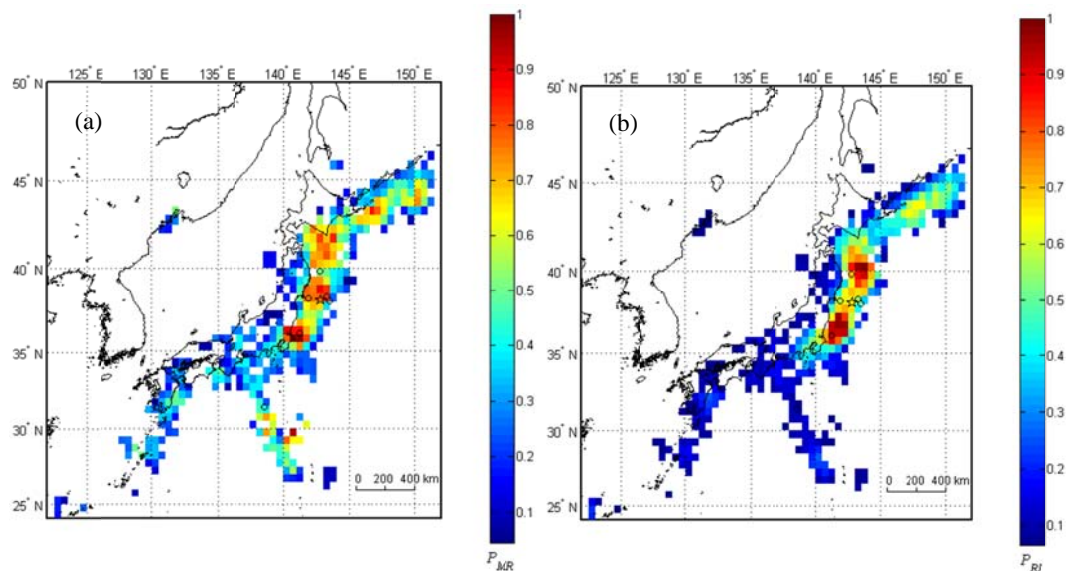


Figure 2. Molchan error diagram for test 2 obtained using (a) uniform and (b) RI weighted spatial priors.

3.3. Test 3 (Prediction of the Tohoku earthquake)

This test aims to test whether the MR method can predict the 2011 M_w 9.0 Tohoku earthquake and its foreshock occurred 2 days before (n° 18) and the $M7+$ earthquakes occurred after the Tohoku earthquake (n° 19), including the large $M7+$ aftershocks (Table 1). The training period starts in January 1st 1890 and ends 7 days before the occurrence of the mainshock, i.e. March 4th 2011. The testing period starts on March 4th 2011 and ends on March 31st 2012. There are 7 $M7+$ target events in the testing region formed by 380 cells. A total of 1795 $M6+$ earthquakes were used in the calculation of the MR and RI alarm functions, from which 1472 occurred in the testing region during the learning period. Here the alarm time step is the whole testing period $\Delta t \approx 1$ year.

Fig. 3a and b show MR and RI forecast maps. The circles and the star show the $M7+$ target earthquakes. Clearly, the MR map catches the Tohoku earthquake in a hot spot whereas RI map fails. This is confirmed from the plot of the $MR \geq 0.7623$ and $RI \geq 0.7204$ optimal maps in Fig. 3c and d. The optimal RI forecast map is plotted with a space-time alarm rate equivalent to the MR optimal map, namely the space time alarm rate $(22/380) = 0.0579$ for MR and $(23/380) = 0.0605$ for RI. MR outscores RI with a miss rate equal to $3/7$ (n° 19p, 22 and 23 are missing), against $6/7$ for the RI map.



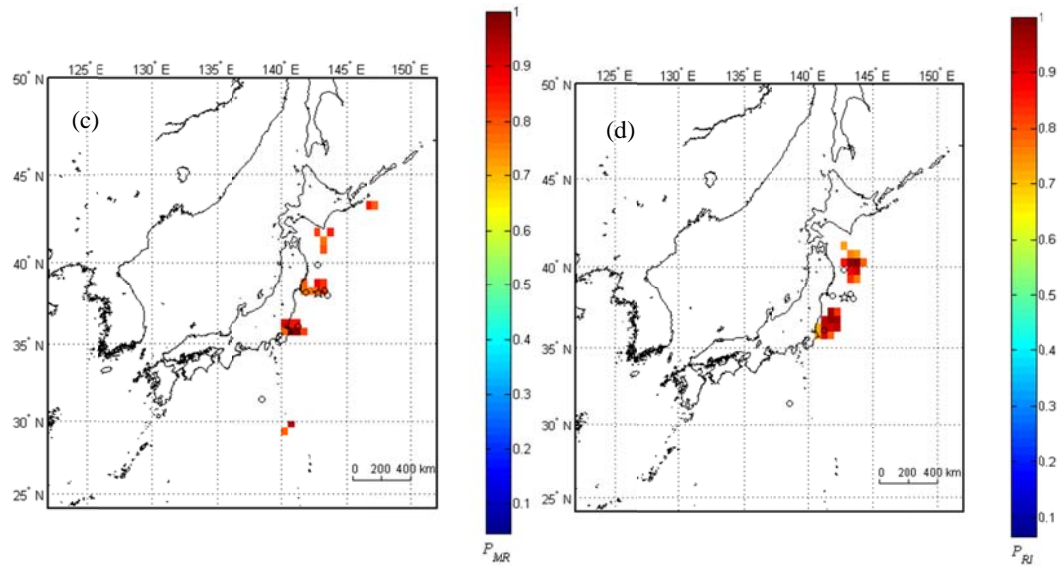


Figure 3. (a) MR and (b) RI forecast maps plotted 7 days before the occurrence of the Tohoku earthquake shown as a star. Optimal (c) MR and (d) RI forecast maps, corresponding to the minimal MR forecasting error.

4. CONCLUSION

This study proposes and tests a new statistics of inter-event times called moment ratio (MR) as a precursory alarm function to forecast large events in Japan. MR is defined by the ratio of the mean over the variance. The forecasting performance of MR was evaluated using Molchan error diagrams. In order to test the applicability of MR maps in forecasting, we used optimal MR maps obtained by plotting the MR scores above the threshold corresponding to the minimum forecasting error (miss rate + space-time alarm rate).

The retrospective tests conducted in this study show that MR outscores both random guessing and the RI method. In the long term, the optimal MR maps succeed in predicting 15 of the 18 M7+ shallow events that occurred in the testing region during the last two decades (1993-2011), with a space-time alarm rate as small as about 20% of the total space-time alarms. In addition, MR reduces the missing rate of shallow events by about 60 % comparing to the RI method. At short term, MR succeeds quite well to predict the 2011 Mw 9.0 Tohoku earthquake, its M7.3 foreshock occurred 3 days earlier and its following M7+ aftershocks, with a very small space-time alarm rate less than 6% of the total space-time alarm region, while the RI method fails. The presence of hot cells very close to missing target earthquakes suggests that MR may be improved by smoothing. The obtained results imply that MR is an alternative forecasting method with good potential skills in forecasting large earthquakes.

ACKNOWLEDGEMENT

This work was supported by a fellowship from the Japanese Society for the Promotion of Science.

REFERENCES

- Corral, A. (2003). Local distributions and rate fluctuations in a unified scaling law for earthquakes. *Phys. Rev. E* **68**, doi:10.1103/PhysRevE.68.035102.
- Hainzl, S., Scherbaum, F. and Beauval, C. (2006). Estimating background activity based on interevent-time distribution. *Bull. Seismol. Soc. Am.* **96**:1, 313–320.
- Joliffe, I.T. and Stephenson, D.B. (Eds.) (2003). *Forecast verification: A practitioner's guide in atmospheric Science*. John Wiley and Sons, England.

- Keilis-Borok, V. (2002). Earthquake prediction: State-of-the-art and the emerging possibilities. *Annu. Rev. Earth. Planet. Sci.* **30**, 1–33.
- Molchan, G. (1997). Earthquake prediction as a decision making problem. *Pure Appl. Geophys.* **149**, 233–247.
- Molchan, G. (2010). Space-time earthquake prediction: The error diagrams. *Pure Appl. Geophys.* **167**, 907–917.
- Molchan, G. and Keilis-Borok, V. (2008). Earthquake prediction: probabilistic aspect. *Geophys. J. Int.* **173**, 1012–1017.
- Nanjo, K. (2010). Earthquake forecast for Italy based on the RI algorithm. *Annal. Geophys.* **53:3**, 117–127.
- Talbi, A. and Yamazaki, F. (2010). A mixed model for earthquake inter-event times. *J Seismol.* **14**, 289–307.
- Tiampo, K.F., Rundle, J.B., McGinnis, S., Gross, S. J. and Klein, W. (2002). Mean field threshold systems and phase dynamics: an application to earthquake fault systems, *Europhys. Lett.* **60:3**, 481–487.
- Tiampo, K.F. and Shcherbakov, R. (2012). Optimization of seismicity based forecasts. *Pure Appl. Geophys.*, doi: 10.1007/s00024-012-0457-9.
- Zechar, J. D. and Jordan, T. H. (2008). Testing alarm-based earthquake predictions. *Geophys. J. Int.* **172**, 715–724.